Spectroscopy, Reims, France, 1972 (unpublished).
[8]E. Anastassakis, A. Pinczuk, E. Burstein, F. H. Pollak, and M. Cardona, Solid State Commun. **8**, 133 (1970).
[9]F. Cerderia, C. J. Buchenauer, F. H. Pollak, and M. Cardòna, Phys. Rev. B **5**, 580 (1972).
[10]A brief report is given in S. Venugopalan and A. K. Ramdas, Bull. Am. Phys. Soc. **18**, 75 (1973).
[11]L. Couture and J. P. Mathieu, C.R. Acad. Sci. (Paris) **224**, 1217 (1947).
[12]R. S. Krishnan and P. S. Narayanan, Indian J. Pure Appl. Phys. **1**, 196 (1963). See also, R. Srivastava, H. V. Lauer, Jr., L. L. Chase, and W. E. Bron, Phys. Lett. A 36, 333 (1971).
[13]S. Venugopalan and A. K. Ramdas, Phys. Rev. B **5**, 4065 (1972).
[14]Harshaw Chemical Co., Crystal Solid State Department, 1945 E. 97th St., Cleveland, Ohio 44106.
[15]Isomet Corp., 103 Bauer Drive, Oakland, N.J. 07436.
[16]V. J. Tekippe, H. R. Chandrasekhar, P. Fisher, and A. K. Ramdas, Phys. Rev. B **6**, 2348 (1972).
[17]A. A. Ballman, J. Cryst. Growth **1**, 37 (1967).
[18]P. V. Lenzo, E. G. Spencer, and A. A. Ballman, Appl. Opt. **5**, 1688 (1966).
[19]A. Feldman, W. S. Brower, Jr., and D. Horowitz, Appl. Phys. Lett. **16**, 201 (1970).
[20]Manufactured by Osram Co., Berlin, Germany. The calibration wavelengths are taken from *Handbook of Chemistry and Physics*, 43rd ed., edited by C. D. Hodgman (Chemical Rubber Publishing Co., Cleveland, 1961), p. 2929.
[21]Westinghouse Electric Corp., Electronic Tube Division, Elmira, N.Y. 14902. The calibration wavelength was taken from the source cited in Ref. 20, p. 2916.
[22]H. S. Peiser, J. B. Wachtman, Jr., and R. W. Dickson, J. Res. Natl. Bur. Stand. (U.S.) A **67**, 395 (1963).
[23]A. A. Kaplyanskii, Opt. Spektrosk. **16**, 1031 (1964) [Opt. Spectrosc. **16**, 557 (1964)].
[24]S. Rodriguez, P. Fisher, and F. Barra, Phys. Rev. B **5**, 2219 (1972). In the present paper we follow the approach outlined in this reference.
[25]E. P. Wigner, *Group Theory and its Application to the Quantum Mechanics of Atomic Spectra* (Academic, New York, 1959), Sec. 4, p. 115.
[26]See, also, S. Ganesan, A. A. Maradudin, and J. Oitmaa, Ann. Phys. (N.Y.) **56**, 556 (1970); E. Anastassakis and E. Burstein, J. Phys. Chem. Solids **32**, 313 (1971); J. Phys. Chem. Solids **32**, 563 (1971). These authors have arrived at the secular equation in Refs. 23 and 24 by starting with the dynamical matrix; it can be shown that the two procedures are equivalent.
[27]J. F. Nye, *Physical Properties of Crystals* (Oxford U. P., Oxford, England, 1964).
[28]See Ref. 27, p. 92.
[29]R. Loudon, Adv. Phys. **13**, 423 (1964).
[30]This is an assumption which has to be verified experimentally. See, for example, Ref. 9, where it is found that this is true for the III-V compounds investigated, but not for the II-VI compound ZnSe.
[31]D. R. Huffman and M. H. Norwood, Phys. Rev. **117**, 709 (1960). The elastic constants given here for 4.2 °K have been used by us. The elastic constants do not vary strongly with temperature and the changes between 4.2 and ≈15 °K are neglected.
[32]D. Gerlich, Phys. Rev. **135**, 1331 (1964); we use the elastic constants given here extrapolated to 0 °K. See comment under Ref. 31.
[33]The unpublished results of S. S. Mitra are quoted by J. R. Ferraro, H. Horan, and A. Quattrochi, J. Chem. Phys. **55**, 664 (1971). We have assumed that Mitra has taken compressive hydrostatic stress to be positive in sign.
[34]M. Onoe, A. W. Warner, and A. A. Ballman, IEEE Trans. Sonics Ultrason. **14**, 165 (1967).
[35]Due to a typographical error, the position of this line is incorrectly given as 97.2 cm^{-1} in Table V of Ref. 13.
[36]B. Kh. Bairamov, B. P. Zakharchenya, and Z. M. Khashkhozhev Fiz. Tverd. Tela **14**, 1374 (1972) [Sov. Phys.-Solid State **14**, 1181 (1972)].
[37]B. Kh. Bairamov, B. P. Zakharchenya, R. V. Pisarev, and Z. M. Khashkhozhev, Fiz. Tverd. Tela **13**, 3366 (1971) [Sov. Phys.-Solid State **13**, 2827 (1972)].
[38]N. Krishnamoorthy and V. Soots, Can. J. Phys. **50**, 1350 (1972).
[39]M. M. Elcombe and A. W. Pryor, J. Phys. C **3**, 492 (1970).
[40]J. P. Hurrell and V. J. Minkiewicz, Solid State Commun. **8**, 463 (1970).
[41]R. Srinivasan, Proc. Phys. Soc. Lond. **72**, 566 (1958).
[42]S. Ganesan and R. Srinivasan, Can. J. Phys. **40**, 74 (1961).
[43]J. D. Axe, Phys. Rev. **139**, 1215 (1965).

PHYSICAL REVIEW B VOLUME 8, NUMBER 2 15 JULY 1973

Resonant Second-Harmonic Generation in the Exciton Region of CuCl and ZnO†

D. C. Haueisen* and H. Mahr
Laboratory of Atomic and Solid State Physics, Cornell University, Ithaca, New York 14850
(Received 10 January 1973)

Using a pulsed tunable dye laser pumped by a Q-switched ruby laser, the frequency dependence of second-harmonic generation has been measured in the region of the first and second 1s excitons of CuCl from about 3.18 to 3.34 eV and the region of the C exciton of ZnO from about 3.38 to 3.48 eV. From the data, the frequency dependence of the optical nonlinear susceptibility has been determined using linear optical constants calculated by a Kramers-Krönig analysis of reflectivity. The results for the single nonzero term of the nonlinear susceptibility of CuCl and the two terms d_{zzz} and d_{zxx} of ZnO have been fit theoretically by an anharmonic-oscillator model employing two oscillators.

I. INTRODUCTION

The intent of the work described here was to experimentally measure the frequency dependence of optical-second-harmonic generation and then to deduce from the data the frequency dependence of the nonlinear optical susceptibility. The measurements were made for second-harmonic light gen-

erated in a frequency region of intrinsic electronic absorption in a crystalline sample where the linear optical susceptibility shows a strong resonant effect to determine if similar resonant dispersion can be observed in the nonlinear response.

Although many measurements of the nonlinear susceptibility in a variety of substances have been made, relatively few experimental results have been obtained on the frequency dependence.[1-8] And of these measurements of nonlinear dispersion, the initial report to come out of the experiments described here[6] represents the only published investigation in the region of a single isolated electronic resonance, which is probably the simplest case to describe theoretically. The early paper by Faust and Henry[2] and very recent work by Levenson, Flytzanis, and Bloembergen[8] investigated nonlinear dispersion of a single resonance in the restrahl region.

Although experimental results have been lacking, theories of the nonlinear susceptibility have been formulated along various lines. The earliest theories, particularly that by Armstrong *et al.*,[9] developed a semiclassical approach with the interaction between the electromagnetic field and the crystal used in a second-order perturbation theory treatment. Seemingly more correct theories of Ovander[10] and Lang[11] have since then been developed which include the lowest-order terms in the crystal-field interaction in describing the unperturbed normal modes of the system. However, the damped anharmonic oscillator[12] provides by far the simplest approach to nonlinear dispersion in a strictly classical manner analogous to the derivation of the linear susceptibility of gases using the harmonic-oscillator model. From the existence of these several approaches, then, experimental data for a simple case of nonlinear resonance dispersion are desirable.

In the work described here the exciton absorption bands of CuCl and ZnO were chosen for the experiments for two primary reasons: First, the need for a sharp, isolated resonance to keep the analysis of the experiment as simple as possible is fulfilled, especially in the case of CuCl where the first $1s$ exciton is sharp and well separated at low temperatures from other excitons and the band edge. The second reason for the particular choice of these substances was the amount of information already available. Numerous studies have been done on the linear and nonlinear optical properties of CuCl[13-20] and ZnO.[21-27]

A. Theory of Optical-Second-Harmonic Generation

Nonlinear optical properties of crystalline solids can be understood (in lowest order) in terms of an induced polarization in the solid which is quadratic in the electric field amplitude inside the solid. The polarization in a solid, then, including the nonlinear effect, is given by

$$\vec{P} = \chi \vec{E} + d\vec{E}\vec{E}, \tag{1}$$

where χ is a second-rank tensor and gives the usual linear response, and d is the nonlinear susceptibility, represented by a third-rank tensor.[28]

To derive a quantitative expression for second-harmonic generation, the nonlinear polarization source term of (1) is introduced into Maxwell's equations for a propagating second-harmonic plane wave. If the fundamental electric field is taken as $E_0 e^{i(\vec{k}\cdot\vec{r}-\omega t)}$, the nonlinear polarization is given by

$$P_i^{\mathrm{NL}} = d_{ijk} E_{0j} E_{0k} e^{2i(\vec{k}\cdot\vec{r}-\omega t)} \ . \tag{2}$$

This polarization can now be introduced into the wave equation including source terms and dissipative terms for a propagating plane wave at the second-harmonic frequency where the second-harmonic field amplitude is a function of distance along the direction of propagation.[29]

However, for the case including absorption at the second-harmonic frequency, a more direct approach can be used. In particular if $\alpha l \gg 1$ where α is the absorption at the second-harmonic frequency and l is the sample length, the second-harmonic wave reaches a steady state inside the crystal where the nonlinear generation of the wave is balanced by absorption of the radiated field. To attain this steady state, it is necessary that the generation of the wave be constant in space and time. This is true if it is assumed that the fundamental field remains constant in amplitude throughout the crystal, that is, if only a small part of the fundamental power is converted to second harmonic, a situation which is realized in nearly all cases. With the fundamental driving electric field described by k and ω, the second-harmonic wave, in this case, has wave vector $2k$ and not the usual $k_{\mathrm{SH}} = (2\omega/c)n_{\mathrm{SH}}$, the wave vector of a freely propagating wave with frequency 2ω, where n_{SH} is the index of refraction at the second-harmonic frequency.

When the second-harmonic-generation problem is solved with the fundamental wave incident on the crystal boundary,[30,31] two second-harmonic waves are found to propagate inside the crystal. To satisfy boundary conditions both a free wave with wave vector k_{SH} and a forced wave with wave vector $2k$ are needed. These correspond to the solutions to the homogeneous and inhomogeneous wave equations, respectively, for the wave at frequency 2ω inside the crystal. The equation which describes second-harmonic propagation is inhomogeneous due to the driving nonlinear polarization source term and the solution to the equation is a combination of solutions to the inhomogenous as well as homogeneous equations. However, in the case considered, where $\alpha l \gg 1$, the free wave which originates at the

boundary is rapidly damped and only the forced wave remains. Under these conditions, then, a steady-state amplitude for the second-harmonic wave is obtained.

The wave equation for this "forced" second-harmonic wave is then

$$[-(2k)^2+(2\omega/c)^2]\vec{E}_{SH} = -4\pi(2\omega/c)^2\vec{P}_{SH}\,, \tag{3}$$

where $\vec{E}_{SH}$ and $\vec{P}_{SH}$ have time and spatial dependence $e^{2i(\vec{k}\cdot\vec{r}-\omega t)}$. The polarization is given by a term linear in $\vec{E}_{SH}$ plus the nonlinear term given in (1):

$$\vec{P}_{SH} = \chi\vec{E}_{SH} + d\vec{E}_0\vec{E}_0. \tag{4}$$

Combining (3) and (4) and dropping vector notation for simplicity

$$[-(2k)^2+(2\omega/c)^2(1+4\pi\chi)]E_{SH} = -4\pi(2\omega/c)^2 dE_0E_0\,. \tag{5}$$

Finally,

$$E_{SH} = \frac{-4\pi(2\omega/c)^2 dE_0E_0}{-(2k)^2+(2\omega/c)^2(1+4\pi\chi)}\,. \tag{6}$$

The denominator in (6) can be written

$$(2\omega/c)^2(\tilde{n}_{SH}^2 - n_F^2), \tag{7}$$

where n_F is the index of refraction at the fundamental frequency and $\tilde{n}_{SH}$ is the complex index of refraction for the second-harmonic frequency, allowing for absorption of the second-harmonic field. It is assumed there is negligible absorption of the fundamental wave.

The second-harmonic power is proportional to $E_{SH}E_{SH}^*$ which is then given by, using (7),

$$E_{SH}E_{SH}^* = \frac{(4\pi)^2|d|^2|E_0|^4}{|\tilde{n}_{SH}^2 - n_F^2|^2}\,. \tag{8}$$

It should be noted that the denominator of (8) includes the usual "coherence-length" effect found in the more usual derivation of second-harmonic generation which is most useful for nonabsorbing media and referred to previously;

$$|\tilde{n}_{SH}^2 - n_F^2|^2 = (c/2\omega)^2[\Delta k^2 + (\tfrac{1}{2}\alpha)^2]\,|n_{SH}+n_F|^2, \tag{9}$$

where $\Delta k = 2k_F - k_{SH}$.

The coherence length is given by

$$l_{coh} = [\Delta k^2 + (\tfrac{1}{2}\alpha)^2]^{-1/2}. \tag{10}$$

The physical interpretation of the coherence length is that it is the distance over which the generated wave remains in phase with itself. Because of dispersion between the fundamental and second-harmonic waves, the nonlinear polarization will be out of phase with the wave it generates in a distance $\Delta x \simeq 1/\Delta k$. In addition, if absorption is present, a freely propagating wave would be damped out in a distance $\Delta x \simeq 1/\alpha$. These two factors then combine according to (10) to produce the coherence length.

The quantity measured in an experiment is the external second-harmonic power generated inside a crystal. It is necessary, then, to relate the internal macroscopic electric field given in (8) to the external power. Intensity is obtained from the Poynting vector given by $\vec{S} = (c/4\pi)\vec{E}\times\vec{H}$ and multiplied by area for the power. From Maxwell's equations, the electric and magnetic fields are related by $|\vec{E}| = \sqrt{\epsilon}\,|\vec{H}|$. But $\sqrt{\epsilon}$ is the proportionality between the wave vector k and ω/c, that is, $k = \sqrt{\epsilon}\omega/c$. In the case of a forced second-harmonic wave, however, the value of $\sqrt{\epsilon}$ to be used is that for the fundamental wave since the wave vector $2k$ and frequency 2ω are related by the fundamental index of refraction, n_F, where $n = \sqrt{\epsilon}$. A similar question arises as to the necessity of correcting for reflectivity of second-harmonic light as it emerges from the back surface of the crystal. Again $\sqrt{\epsilon}$ is the factor which determines reflectivity since the tangential components of $\vec{E}$ and $\vec{H}$ are continuous across the boundary. With $\sqrt{\epsilon} = n_F$ again, the external second-harmonic power is given by

$$P_{SH} = |E_{SH}|^2\,\frac{c}{4\pi}\,n_F(1-R)A = \frac{(4\pi)^3|d|^2P_0^2(1-R)}{|\tilde{n}_{SH}^2 - n_F^2|^2 n_F cA}\,, \tag{11}$$

where P_0 is the fundamental power inside the crystal, A is the area of the beam, and R is the reflectivity at the back surface given by $R = (n_F-1)^2/(n_F+1)^2$.

In the experiments, the fundamental frequency was in a region where the crystal is transparent while the second harmonic was in a region of intrinsic electronic absorption, in particular, in the exciton region just below the band-to-band transition edge. Since only relative second-harmonic power was measured, the factors involving R and n_F are unimportant because they relate to the optical constants of the fundamental wave which show very little dispersion in the region of interest. This point is made only because it would seem correct to relate P_{SH} to E_{SH} and reflectivity with the optical constants associated with the second-harmonic wavelength. If that were the case, large fluctuations in P_{SH} would be introduced in a region of intrinsic absorption of P_{SH} owing to the resonant effect on the linear optical constants. But such is not the case and, therefore, the equation of interest in comparing theory and experiment is

$$P_{SH} \propto \frac{|d|^2P_0^2/A}{|\tilde{n}_{SH}^2 - n_F^2|^2}\,. \tag{12}$$

B. Anharmonic-Oscillator Model of the Nonlinear Susceptibility

There are several methods, both classical and quantum mechanical, which can be used to find a specific form for the nonlinear susceptibility d as

mentioned at the beginning of this section. The simplest model that can be constructed is one which is the logical extension of the simplest model available to calculate the linear susceptibility, i.e., the harmonic oscillator generalized to the nonlinear case in terms of the anharmonic oscillator.[12]

The solid is considered to be an ensemble of fixed, independent, anharmonic oscillators driven by an externally applied electromagnetic field. The equation of motion then reads

$$\ddot{x} + \omega_0^2 x + \Gamma\dot{x} + \omega_0^2 v x^2 = (e/m)E(\omega). \tag{13}$$

For simplicity only one resonance of frequency ω_0 is assumed and damping is included as a term proportional to the velocity of the displacement with Γ/ω_0 a unitless quantity. The nonlinear coupling constant $\omega_0^2 v$ is defined such that v has dimensions of reciprocal length and is considered small in the sense that v is much less than the reciprocal of the maximum displacement of the oscillator. In zeroth order (neglecting the quadratic term) the familiar form of a complex linear susceptibility results from (13):

$$\chi(\omega) = \frac{Nfe^2/m}{\omega_0^2 - \omega^2 - i\Gamma\omega}, \tag{14}$$

where N is the number of oscillators per unit volume and f is the oscillator strength. The complex dielectric constant is as usual

$$\tilde{\epsilon}(\omega) = 1 + 4\pi\chi = 1 + \frac{4\pi Nfe^2/m}{\omega_0^2 - \omega^2 - i\Gamma\omega}. \tag{15}$$

Then including the nonlinear term, to first order in $\omega_0^2 v$, there is a displacement at 2ω:

$$x(2\omega) = \frac{\omega_0^2 v (e/m)^2 E^2(\omega)}{[\omega_0^2 - (2\omega)^2 - i2\omega\Gamma](\omega_0^2 - \omega^2 - i\Gamma\omega)^2}. \tag{16}$$

The polarization associated with this displacement is $P(2\omega) = Nf_{\mathrm{NL}} e x(2\omega)$ where f_{NL} is a nonlinear oscillator strength, and the nonlinear susceptibility for second-harmonic generation at 2ω is given by

$$d(2\omega) = \frac{\omega_0^2 v N f_{\mathrm{NL}} e^3/m^2}{[\omega_0^2 - (2\omega)^2 - i2\omega\Gamma](\omega_0^2 - \omega^2 - i\omega\Gamma)^2}$$

$$= \frac{A\omega_0^2}{[\omega_0^2 - (2\omega)^2 - i2\omega\Gamma]}, \tag{17}$$

$$A = \frac{vNf_{\mathrm{NL}} e^3/m^2}{(\omega_0^2 - \omega^2 - i\omega\Gamma)^2}.$$

This microscopic nonlinearity can be converted into macroscopic quantities using effective or local-field corrections.[28]

In the experiments considered here where the fundamental frequency is far from the resonant frequency ω_0, the resonant denominator $\omega_0^2 - \omega^2$ in (17) is unimportant and included in the defined constant A.

The nonlinear susceptibility can also be expressed in terms of the linear susceptibility [Eq. (14)]:

$$d(2\omega) = \frac{\omega_0^2 v f_{\mathrm{NL}} \chi^2(\omega)}{eNf^2[\omega_0^2 - (2\omega)^2 - i2\omega\Gamma]}. \tag{18}$$

It can be seen that off resonance, i.e., for $2\omega \ll \omega_0$, the quantity $\delta = d(2\omega)/\chi^2(\omega)$ is constant (and nearly the same for many substances: Miller's rule[32]). With the second harmonic nearly resonant, $\omega_0 \approx 2\omega$, as in the experiments reported here, the resonant denominator $[\omega_0^2 - (2\omega)^2 - i2\omega\Gamma]$ does have a significant effect and it was the object of these experiments to try to observe *that* nonlinear resonant dispersion.

It is clear that the model presented above could be improved in several ways, most notably by allowing coupling between oscillators which leads to theories of spatial dispersion. It is the objective of this paper to test the simple model first against experimental evidence. More sophisticated theories and their comparison with the same experimental results will be taken up in a separate paper.

II. EXPERIMENTAL DESIGN

In order to do second-harmonic generation as a function of frequency, a tunable laser source is central to the necessary apparatus. Organic dyes pumped by a strong light source exhibit broad-band emission and provide an active medium for such a tunable laser. The dye laser, then, along with other optical apparatus and cryogenics capable of helium temperature form the basic experimental equipment used in the studies reported here.

A. Tunable Organic Dye Laser

Pulsed laser emission from an organic dye was first reported by Sorokin and Lankard[33] in 1966. Since that time hundreds of dyes have been observed to exhibit laser action with output wavelengths covering the entire visible spectrum.[34]

Figure 1 shows a schematic of the dye laser used in the present experiments. The dissolved dye is contained in a 1×1-cm cell which is about 4-cm high. The optical cavity is formed by the output reflector and a diffraction grating. A dielectrically coated mirror with reflectivity of 90% mounted in a gimbal Lansing device serves as the output reflector. Because of the high gain of the dye under pulsed pumping conditions, this output mirror reflectivity can be as low as 30% for most dyes without significant change in the output power. The grating used for the other cavity reflector is an 1800 line per mm Bausch and Lomb plane grating, blazed for 5000 Å. This grating functions as the wavelength selector for the laser[35] by reflecting a single wavelength in first order back down the axis of the optical cavity to be amplified. Such a narrow-band feedback device caused the laser to os-

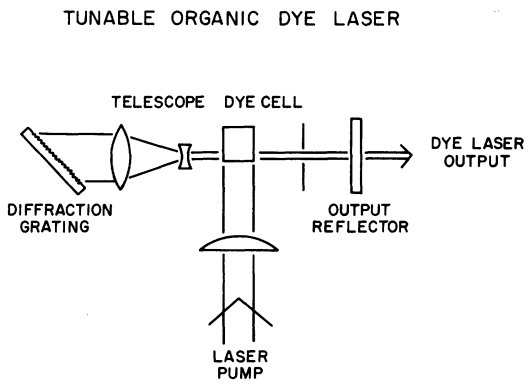

FIG. 1. Schematic of the tunable dye-laser configuration.

cillate in only a very small portion of the broad luminescence spectrum. Rotation of the grating, then, provides tuning of the laser by varying the feedback wavelength. The grating is also located in a Lansing mount to facilitate alignment and precise wavelength selection.

The telescope inside the dye-laser cavity serves two functions. It prevents burning of the grating with some dyes where the power generated in the cavity is especially high. Also, it spreads the beam over most of the 3×3-cm area of the grating improving resolution, thereby producing a narrower output linewidth. No direct measurements of the linewidth were made but resolved structure in the data indicates it is typically less than 1 Å with this configuration.

The aperture just behind the output reflector serves to limit the divergence of the laser and suppress extraneous cavity modes. The dye cell and telescope provide reflecting surfaces which can give rise to these extra modes. The dye cell is positioned just off the vertical direction so that the mode between the dye cell walls will not pass through the aperture and be observed at the output.

Finally, the pumping source for the dye used in these experiments was the output of a pulsed ruby laser, a TRG model No. 104, Q switched by a rotating prism. Typical pumping power was 10–20 MW for about a 20-nsec pulse. The ruby-laser output was focused by a cylindrical lens of approximately 10-cm focal length onto the dye cell.

The output of the dye laser used in this study was typically of the order of 100 kW for a 10–20 nsec pulse. A primary difficulty of the output was the mode characteristics, complicated in the present case by some of the particular dyes used, as already indicated. Because of the proximity of the laser wavelength region needed for these experiments at about 7000–8000 Å and the ruby-laser pumping wavelength at 6943 Å, the pumping was done at the edge of the absorption band of the dyes and necessitated dye solutions of relatively high concentration. The optical density of the 1-cm cell had to be as high as 8–10 to get laser action in some cases. Hence, most of the pumping light was absorbed in less than 1 mm at the front of the cell, making a small beam waist for the dye laser and complicating alignment, leading to the poor mode characteristics of the output. In other dyes where pumping is more convenient and dye cells of optical density around one to two are used, this problem is observed to be significantly reduced.

The dyes used in these experiments were determined by the exciton energies in CuCl and ZnO since the object was to do second-harmonic generation in a region of intrinsic electronic absorption, for which the excitons of CuCl and ZnO were chosen. Excitons in both these substances are found in the region from about 3.2 to 3.4 eV, which corresponds to a wavelength of 3900–3600 Å. This means a fundamental wavelength of 7800 Å is required. Three dyes used to produce these wavelengths are listed in Table I. All were pumped with fundamental ruby-laser radiation.

B. Second-Harmonic Generation

Figure 2 shows the experimental apparatus used to make second-harmonic-generation measurements. The output of the dye laser, described in Sec. II A, is focused onto the sample mounted in a cryostat. The CuCl samples were placed in a helium-conduction cryostat which cooled them to about 20°K while an immersion cryostat was used for the ZnO samples, the temperature going to about 1.8°K in this case while pumping on the helium. Second-harmonic light from the sample was passed through a model No. 82-000 Jarrell-Ash $\frac{1}{2}$-m monochromator and detected with a Dumont 6292 photomultiplier (S11 spectral response). The monochromator along with the optical filter at the input discriminated against laser light. Also the monochromator was used to discriminate against two-photon induced luminescence in wavelength regions where significant luminescence was generated.

For a reference, part of the dye-laser output was split off and passed through a non-phase-matched ($\Delta k \neq 0$) ammonium dihydrogen phosphate (ADP)

TABLE I. List of dyes used with the dye laser.

Dye	Solvent	Optical density	Laser wavelength (Å)
Brilliant green	glycerin	≃9	7300–8300
Naphthalene green V	glycerin	4	7500–7800
Diethylthiadicarbocyanine iodide (DTDC)	ethylene glycol	4	7000–7700

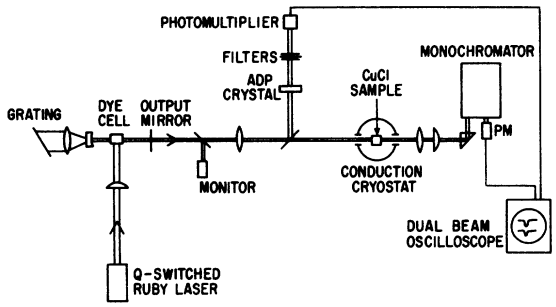

FIG. 2. Experimental arrangement for second-harmonic-generation (SHG) measurements using SHG from ADP as a reference.

crystal.[36] Second-harmonic light from the ADP was then detected using another Dumont 6292 photomultiplier. Optical filters eliminated laser light and one short-wavelength cutoff filter was placed ahead of the ADP to ensure that light of about the second-harmonic wavelength did not enter the detector system. This form of reference was chosen over simply sampling the dye-laser output since the area of the focal region of the dye-laser enters into (12) relating the fundamental and second-harmonic power. Because of poor mode structure, this area probably varied from one pulse to the next and also as the laser was tuned over a large wavelength region. Furthermore, it was assumed that the second-harmonic generation efficiency in ADP was constant over the wavelength region studied since it was far from any absorption in ADP and the sample was oriented away from phase matching ($\Delta k \neq 0$).

A monitor of the dye-laser beam using a glass plate to sample the beam and a Hewlett Packard 4205 photodiode for detection was included.

The signal and reference was simultaneously recorded using Polaroid pictures taken with type-410 Polaroid film from the trace of a Tektronix 551 dual-beam oscilloscope equipped with type-L fast-rise preamp ($\simeq 10$ nsec).

C. Sample Orientation

CuCl has zinc-blende structure ($43m$) and there is a single independent nonzero term in the nonlinear susceptibility tensor d. Second-harmonic polarization may arise from three terms:

$$P_x = 2d_{xyz}E_yE_z, \quad P_y = 2d_{yzx}E_zE_x, \quad P_z = 2d_{zxy}E_xE_y, \tag{19}$$

with $d_{xyz} = d_{yzx} = d_{zxy}$.

In the experiments the fundamental beam was directed along $\langle 111 \rangle$ directions, generating a nonlinear polarization that is both parallel ("longitudinal") and perpendicular ("transverse") to the direction of propagation. The transverse excitation will give rise to second-harmonic generation. ZnO crystallizes in the hexagonal zincite structure (6 mm), and there are two independent nonzero terms in the nonlinear susceptibility tensor:

$$P_x = 2d_{xxz}E_xE_z, \quad P_y = 2d_{yyz}E_yE_z,$$
$$P_z = d_{zxx}E_xE_x + d_{zyy}E_yE_y + d_{zzz}E_zE_z, \tag{20}$$

where $d_{xxz} = d_{yyz} = d_{zyy} = d_{zxx}$ and d_{zz} is the other independent term. The experiments were done with the direction of propagation of the fundamental beams perpendicular to the c axis and the polarization either parallel (d_{zzz}) or perpendicular (other terms, d_{zxx}, etc). In both cases the second-harmonic polarization is entirely transverse so no longitudinal excitations are excited.

III. EXPERIMENTAL RESULTS

The second-harmonic-generation data were taken for the region of exciton absorption in both CuCl and ZnO. To obtain the nonlinear susceptibility, (12) is used, rewritten below to include second-harmonic-power output from ADP as a reference signal, as described in Sec. II;

$$P_{SH}/P_{ADP} \propto |d|^2/|\tilde{n}_{SH}^2 - n_F^2|^2. \tag{21}$$

The remaining quantities necessary to the analysis are just the simple index of refraction for the fundamental frequency and the complex index of refraction for the second harmonic. In a region of intrinsic absorption, the complex index of refraction is impossible to obtain directly since light will not penetrate even very thin samples where α becomes as large as 10^5 or 10^6 cm^{-1}. For evaporated films, the optical properties may be quite different than the bulk crystal properties which are needed for the analysis. This problem is usually surmounted by doing a Kramers-Krönig analysis of reflectivity measurements.[37] This is, in fact, what was used to obtain the linear optical constants necessary to the analysis of the nonlinear susceptibility in (21).

A. Second-Harmonic-Generation Measurements in CuCl

Figure 3 shows relative second-harmonic generation in CuCl as a function of energy at about 20°K. Two distinct one-photon exciton absorption peaks in this region[14,15] are located at 3.202 and 3.27 eV at helium temperatures. As shown in Fig. 3, there is no distinct structure in the second-harmonic power output at these one-photon absorption peaks. The strong peak in the data at 3.217 eV is a result of a single point of near phase matching ($\Delta k = 0$) along the linear dispersion curve of CuCl where, as a result, the coherence length reaches a local maximum. This phase-matched point occurs between the two exciton absorption peaks where there is large dispersion in the index of refraction, passing through the value of the index for the fundamental at one point providing the phase matching. This is seen clearly in Fig. 4 where a Kramers-

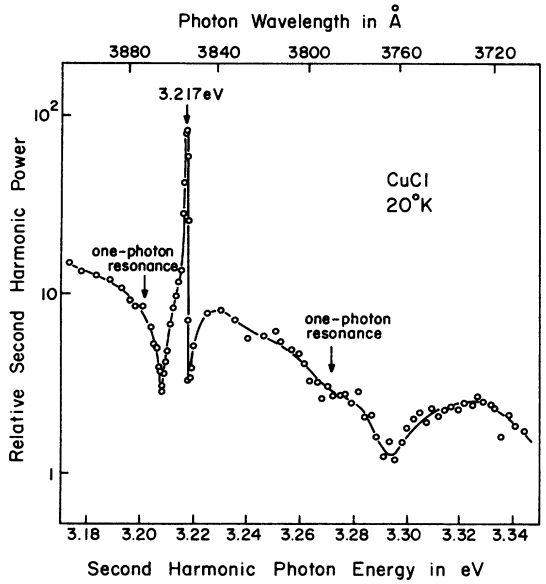

FIG. 3. Relative second-harmonic power output of CuCl as a function of wavelength in the region of the first and second 1s exciton resonances (indicated by arrows).

Krönig analysis of reflectivity done by Staude[38] is shown. At about 3.217 eV the index of refraction has a value of 1.95 which is the approximately constant value of the index for the fundamental[18] shown by the horizontal dashed line. It should also be noted that the absorption in this region is small, allowing the rapid change in Δk around the phase-matching point to have a dominant effect on the coherence length.

The values of the linear optical constants, shown in Fig. 4, were used in (21) to calculate the nonlinear susceptibility. The result is shown by the circles in Fig. 5. In this logarithmic plot of $|d|$ for CuCl, two resonances, centered on the one-photon 1s exciton resonances, are clearly displayed. It

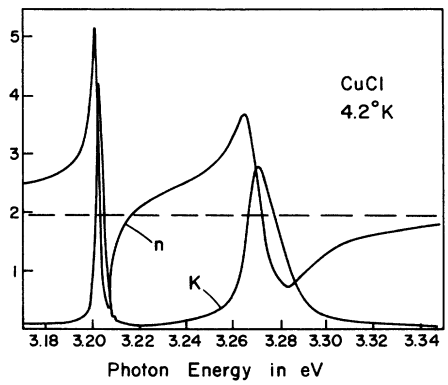

FIG. 4. Linear optical constants of CuCl in the region of the first and second excitons obtained from a Kramers-Krönig analysis of reflectivity.

was previously shown[39] that the first of these resonances can be well described by the predictions for $|d|$ of an anharmonic-oscillator model.

B. Second-Harmonic-Generation Measurements in ZnO

Relative second-harmonic power output in ZnO is shown in Figs. 6(a) and 6(b) for the cases of fundamental beam polarization parallel and perpendicular to the c axis in both cases. There is no absolute scale between the data taken for the two different polarizations. In both cases Eqs. (20) show that the second harmonic is polarized parallel to the c axis since only the third of the equations contains nonzero contributions with the configuration used. This polarization condition was observed in the experiments. The data were taken in the region of the C exciton in ZnO at about 3.42 eV.[21,25] This is the first strong one-photon exciton absorption peak in ZnO for light polarized parallel to the c axis. Two other excitons, called A and B, are located at about 3.38 eV but coupled only by light polarized perpendicular to the c axis. As second-harmonic light is always parallel to the c axis, excitons A and B are not of immediate interest to the experiments described here.

The data of Fig. 8 show very little structure in the second-harmonic power output. With both polarizations a weak local maximum occurs around 3.445 eV which is a result of an increase in the coherence length in that region.

In Fig. 7 the linear optical constants are shown for this energy region of ZnO for light polarized parallel to the c axis. The data are again a result

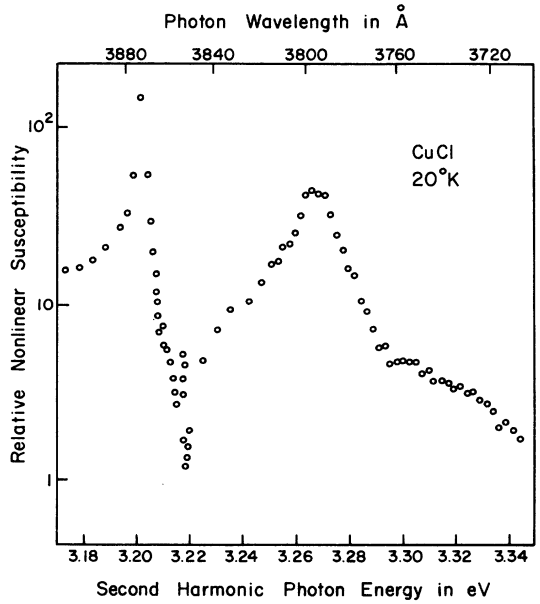

FIG. 5. Relative nonlinear susceptibility of CuCl calculated from SHG data and the linear optical constants.

of a Kramers-Krönig analysis of reflectivity.[40] The straight broken lines in Fig. 7 at about $n = 2$ give the ordinary and extraordinary indices of refraction at the fundamental frequency[41] which produces second harmonic in this region. From Fig. 7, then, it is clear that the coherence length does have a maximum in the region of 3.445 eV where the absorption goes through a minimum and near phase matching is achieved, although the peak in second-harmonic power output is not nearly as pronounced as the maximum observed at the phase-matching point in CuCl. This lack of a sharp peak in ZnO is a result of the coherence length not being strongly dominated by phase mismatch in that region. Δk does go through several orders of magnitude in just a few meV in passing through the phase-matching condition, but absorption apparently remains large enough such that rapid change in Δk does not strongly affect the coherence length as for the first exciton resonance in CuCl.

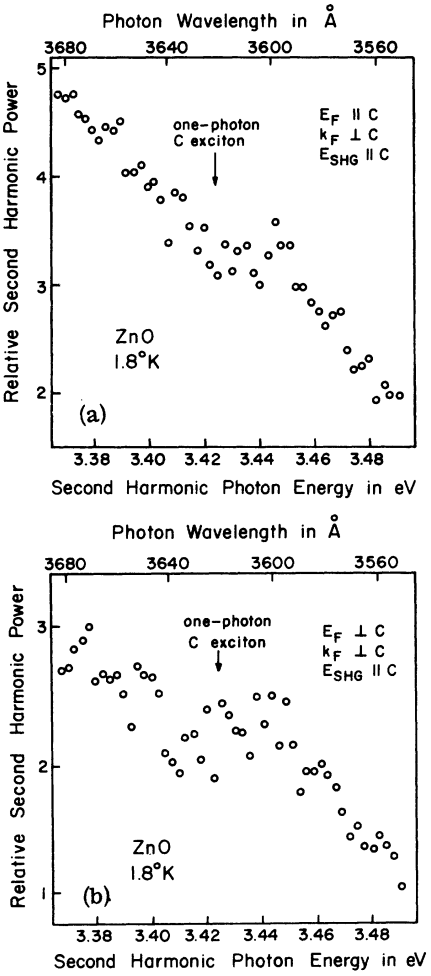

FIG. 6. Relative second-harmonic power output of ZnO in the region of the C exciton for propagation perpendicular to the c axis and (a) with both fundamental and second-harmonic polarization parallel to the c axis (d_{zzz}) and (b) with the fundamental polarization perpendicular to the c axis and the second-harmonic polarization parallel to the c axis (d_{zxx}).

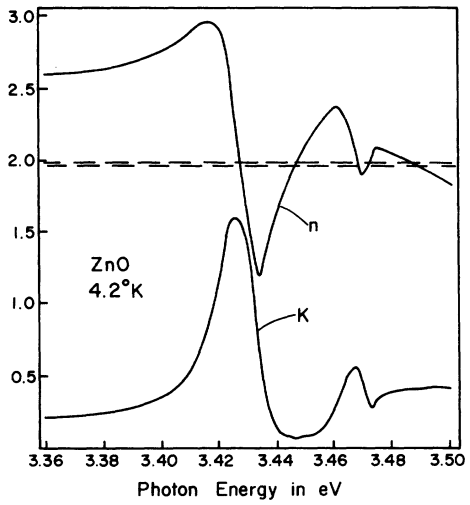

FIG. 7. Linear optical constants of ZnO in the region of the C exciton obtained from a Kramers-Krönig analysis of reflectivity.

Again using (21) and the linear optical data of Fig. 7, the nonlinear susceptibility is calculated for the cases of fundamental polarization parallel and perpendicular to the c axis and the results are shown in Figs. 8(a) and 8(b), respectively. The calculated circles show two resonances in each case, centered on the one-photon resonances of Fig. 7 at about 3.42 (C exciton) and 3.465 eV.

IV. ANHARMONIC-OSCILLATOR-MODEL FIT TO THE NONLINEAR SUSCEPTIBILITY

For CuCl as well as ZnO two resonances of the nonlinear susceptibility are observed. A theoretical fit using the anharmonic-oscillator model outlined in Sec. I was attempted in the following way: It is assumed that the total contribution to the nonlinear susceptibility d is given by the sum (of complex numbers)

$$d(2\omega) = d + d' + d_\infty = \frac{A\omega_0^2}{\omega_0^2 - (2\omega)^2 - i\Gamma\omega} + \frac{A'\omega_0'^2}{\omega_0'^2 - (2\omega)^2 - i\Gamma'\omega} + d_\infty , \quad (22)$$

where d is the contribution of an anharmonic oscillator of frequency ω_0, damping Γ, and nonlinear "strength" $A = (vNf_{NL}e^3/m)/(\omega_0^2 - \omega^2)^2$, [see Eq. (17)] and d' arises from an anharmonic oscillator of frequency ω_0', damping Γ', and "strength" $A' = (v'Nf_{NL}'e^3/m)/(\omega_0'^2 - \omega^2)^2$. Finally d_∞ repre-

sents the (approximate) constant contribution to d from all resonances at higher frequencies. The measured quantity is a relative value of $|d|$. Performing the calculation of $|d|$ from (22) one gets

$$|d| = d_\infty \left(1 + \frac{(A/d_\infty)^2\omega_0^4 + 2(A/d_\infty)\omega_0^2[\omega_0^2 - (2\omega)^2]}{[\omega_0^2 - (2\omega)^2]^2 + (2\omega\Gamma)^2} + \frac{(A'/d_\infty)^2\omega_0'^4 + 2(A'/d_\infty)\omega_0'^2[\omega_0'^2 - (2\omega)^2]}{[\omega_0'^2 - (2\omega)^2]^2 + (2\omega\Gamma')^2}\right.$$
$$\left. + \frac{2(AA'/d_\infty^2)\omega_0^2\omega_0'^2\{[\omega_0^2 - (2\omega)^2][\omega_0'^2 - (2\omega)^2] + (2\omega)^2\Gamma\Gamma'\}}{\{[\omega_0^2 - (2\omega)^2]^2 + (2\omega\Gamma)^2\}\{[\omega_0'^2 - (2\omega)^2]^2 + (2\omega\Gamma')^2\}}\right)^{1/2}. \quad (23)$$

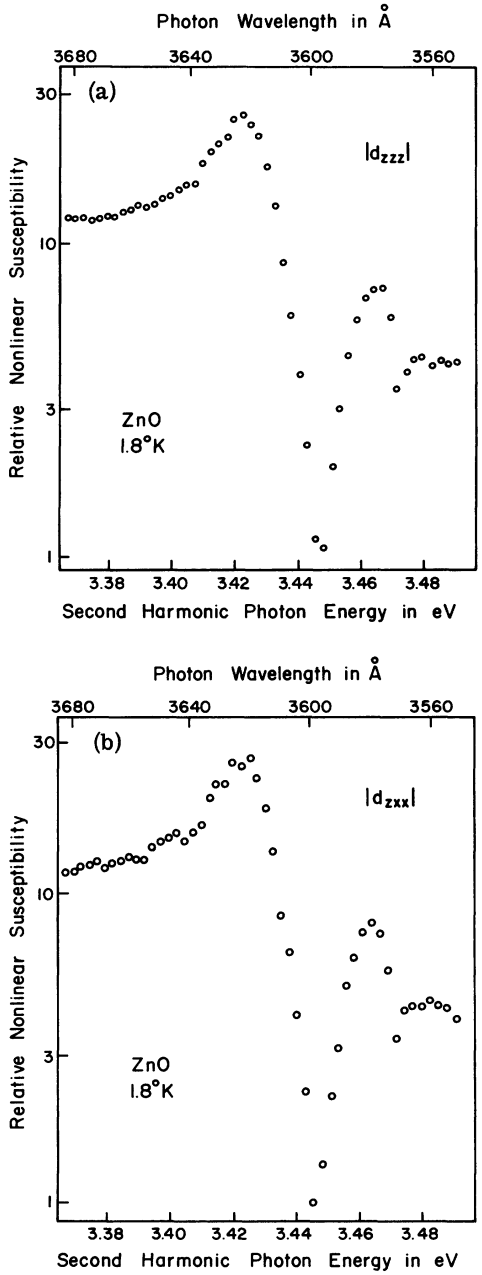

FIG. 8. Relative nonlinear susceptibility of ZnO, (a) d_{zzz} and (b) d_{zxx}, calculated from SHG data and the linear optical constants.

Similarly the linear dielectric constant ϵ for two oscillators is given by

$$\epsilon(2\omega) = \epsilon + \epsilon' + \epsilon_\infty = \frac{B\omega_0^2}{\omega_0^2 - (2\omega)^2 - i\Gamma 2\omega} + \frac{B'\omega_0'^2}{\omega_0'^2 - (2\omega)^2 - i\Gamma' 2\omega} + \epsilon_\infty, \quad (24)$$

$$B = 4\pi N f e^2/m\omega_0^2.$$

An attempt will now be made to fit the observed data of Figs. 3 and 6 as well as the linear optical constants of Figs. 4 and 7 and other available experimental data with a two-oscillator model as expressed by (23) and (24). Using (21) a computer fit was attempted of the original data of Figs. 3 and 6 with six constants A, A', B, B', Γ/ω_0, and Γ'/ω_0', as well as fixed values for ϵ_∞, n_F, ω_0, and ω_0'. After a best fit was obtained, under the constraint that B, B', Γ, Γ', and ω_0, ω_0' would also give a best fit to the linear optical data, these constants were then kept fixed. Using (23) and (24) a calculation of $|d|$ and n and k was done next. Also, using (21) values for $|d|$ were found by multiplying the original data by $|\tilde{n}_{SH}^2 - n_F^2|^2$, where $\tilde{n}_{SH}(2\omega)$ was taken from (24). Figures 9 and 10(a) and 10(b) show the results for $|d|$ for CuCl and ZnO, respectively. The solid lines are computed from (23) with the constants given in the graph. The circles are obtained from the data in a way mentioned above.

In general the fit is very good. For CuCl disagreement is found near two depressions in the original data, near 3.21 and 3.22 eV on both sides of the phase-matched point. The first depression near 3.21 eV could not be fit with a two-oscillator model no matter which constants were used. A fit was obtained after spatial dispersion was included with the two-oscillator model. This will be the subject of discussion in a separate paper.

The bad fit of the solid line to data in Fig. 9 near 3.22 eV is due to the absence of absorption in that wavelength region. Figure 11 shows the linear optical constants calculated from (24) with the constants of Fig. 9. A comparison shows that absorption in the region 3.22–3.24 eV of Fig. 4 that is predicted by the Kramers-Krönig analysis of reflectivity data cannot be accounted for by a simple

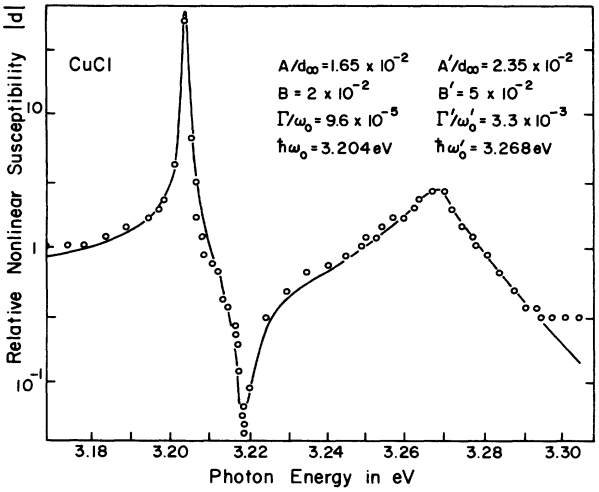

FIG. 9. Relative nonlinear susceptibility of CuCl. The circles represent calculated results from SHG data using the linear optical constants and the solid curve is the theoretical fit. The linear optical constants and the SHG data were fit using the harmonic- and anharmonic-oscillator models, respectively, using two resonant frequencies with self-consistent parameters. The best fit yields the "data" points then calculated from the SHG data and the theoretical curve shown.

oscillator model with one damping constant Γ. For that reason the "data" are lower than they would be in the presence of absorption.

For ZnO [Figs. 10(a) and 10(b)] no perfect fit could be achieved although the solid line drawn with the six constants as given comes very close to the "data" points. The reason is simply that a two-oscillator model of the linear constants of ZnO is a very poor fit to the data as obtained from the Kramers-Krönig analysis of reflectivity. Especially the result of the low energy end of Fig. 7 is in disagreement with direct measurements[26] in such a manner that better data would tend to improve the agreement between experiment and theory for the nonlinear susceptibility.

A comparison of the data (circles) of Fig. 5 with Fig. 9 for CuCl and Fig. 8 with Fig. 10 for ZnO shows the confidence limits of the method used for the determination of $|d|$. Two different means for getting $|d|$ give an overall result that is quite similar. An improvement of the reliability with which one can get $|d|$ certainly depends solely on the reliability of the linear optical data. The theoretical fit of Figs. 10(a) and 10(b) for ZnO was made using almost identical parameters in (23) and (24). This was found to be true although different terms in the nonlinear susceptibility tensor are represented by the two curves, d_{zzz} and d_{zxx}. The absolute values do not correspond. In the transparent region of the crystal d_{zzz} is found to be about three times as large as d_{zxx}.[32] The similarity of the results is explained by noting that the same resonant oscillator is examined in each case since the polarization and direction of propagation of the second-harmonic wave is the same in the two cases.

V. ANALYSIS OF EXPERIMENTAL RESULTS

A comparison between the linear and nonlinear resonances can be made to obtain the value of the nonlinear coupling constant v. As suggested by Miller[32] and derived for the present model by Garrett[42] v can be expressed as [see Eqs. (17) and (18)]

$$v = AeNf^2/\chi^2(\omega) f_{NL} = AeNf/\chi^2(\omega), \tag{25}$$

where $\chi(\omega)$ is the linear optical susceptibility at the fundamental frequency ω, N is the number of oscil-

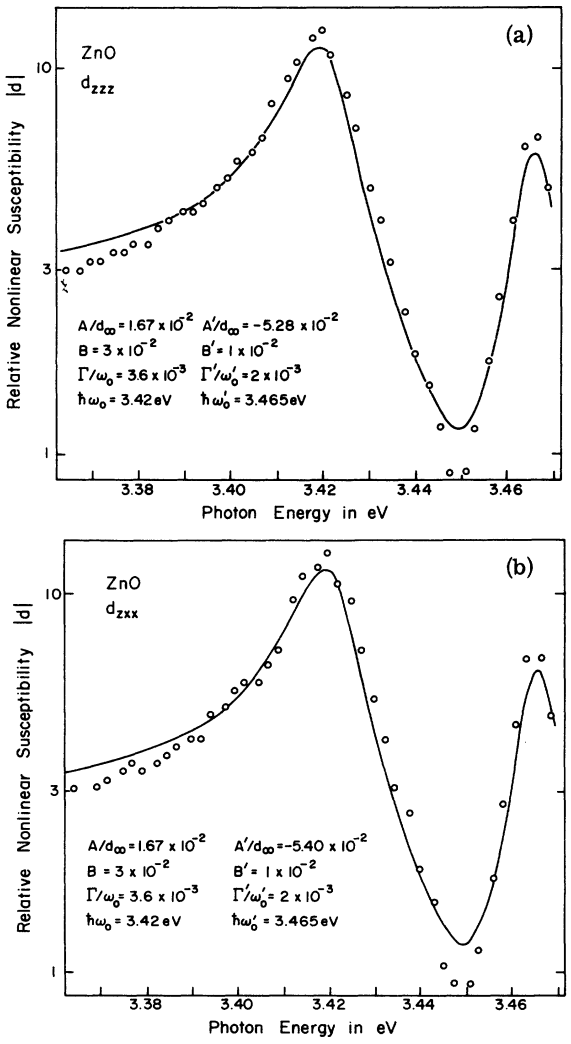

FIG. 10. Relative nonlinear susceptibility of ZnO for components (a) d_{zzz} and (b) d_{zxx}. The circles are calculated "data" points and the solid curve is the theoretical fit. (Analysis similar to CuCl as explained in Fig. 9 caption.)

lators per volume, and e is the electronic charge. The factor f_{NL}/f in (25) must be exactly one. This is because the oscillator strength is the fraction of the total number of oscillators which participate in a given resonance, and this fraction must be the same for both the linear and nonlinear susceptibility since the actual displacement of each of the identical oscillators is in a sense Fourier analyzed to obtain the fundamental and second-harmonic response. In order to get values for v for each resonance we must proceed carefully since our previous analysis results in relative values A/d_∞ and A'/d_∞ only.

For the long-wavelength limit ($\omega \ll \omega_0$) it can be seen from (22) that

$$d_{vis} = d + d' + d_\infty \approx A + A' + d_\infty \tag{26}$$

or

$$\left|\frac{d_{vis}}{d_\infty}\right| = \left|1 + \frac{A}{d_\infty} + \frac{A'}{d_\infty}\right| . \tag{27}$$

With A/d_∞ and A'/d_∞ from Figs. 9 and 10 of the order of 10^{-2} we get that $d_{vis} \approx d_\infty$, i.e., the resonances that we explored here contribute only a few percent to the total value of d in the visible:

$$\left|\frac{d_{vis}}{d_\infty}\right| \approx 1 + \frac{1}{2}\left(\frac{A}{d_\infty} + \frac{A'}{d_\infty}\right) . \tag{28}$$

CuCl: From the best fit of Fig. 9 we obtain $A/d_\infty = 1.65\times10^{-2}$; $A'/d_\infty = 2.35\times10^{-2}$. Hence $|d_{vis}| = 1.02|d_\infty|$ or a 2% increase over both resonances. From (25) we get that $v \approx 5\times10^6$ cm^{-1} and $v' \approx 4\times10^6$ cm^{-1}.

ZnO: From a best fit of Figs. 10(a) and 10(b) we obtain $A/d_\infty = 1.67\times10^{-2}$ and $A'/d_\infty = -5.4\times10^{-2}$. Hence $|d_{vis}| \simeq 1.02|d_\infty|$ or a 2% increase. The values for v are $v(zzz) \approx 3\times10^6$ cm^{-1}, $v(zxx) \approx 1\times10^6$ cm^{-1}, and $v'(zzz) = -3\times10^5$ cm^{-1}, $v'(zxx) = -1\times10^5$ cm^{-1}. Note that A'/d_∞ and v' are negative and that the values of v' are down by about an order of magnitude over the values of v. In the case of ZnO, an important question is the relationship between the resonances in the two different terms of the nonlinear susceptibility tensor d_{zzz} and d_{zxx}. Identical parameters were used in the theoretical fit and this might well be expected since the same direction of polarization and propagation of the second-harmonic wave is present for the two cases, that is, the same oscillator is responsible for generating the second harmonic. The values of d obtained for the two tensor components indicate a difference in the efficiency of driving the oscillator nonlinearly by the different polarization fundamental waves. Indeed, the identical fit to the data in the logarithmic plots of Figs. 10(a) and 10(b) means that the resonant amplitudes scale as the constant values of d_{vis}. From (28) $d_{vis}(zzz)/d_\infty(zzz) = d_{vis}(zxx)/d_\infty(zxx)$ or $d_\infty(zzz)/d_\infty(zxx)$ is approximately the same as their ratio in the visible.

Comparison with phonon resonances: Finally we would like to compare the order of magnitude of A/d_∞ obtained here for excitonic resonances with values obtained in the near infrared with phonon resonances. In GaP Faust *et al.*[2,3] obtained a value of $A/d_\infty = -0.53$ for the restrahl band. Levenson *et al.*[8] found a value of $+0.047$ for a third-order nonlinear resonance in diamond.

VI. SUMMARY

(a) The measurements reported here demonstrate that second-harmonic generation can reli-

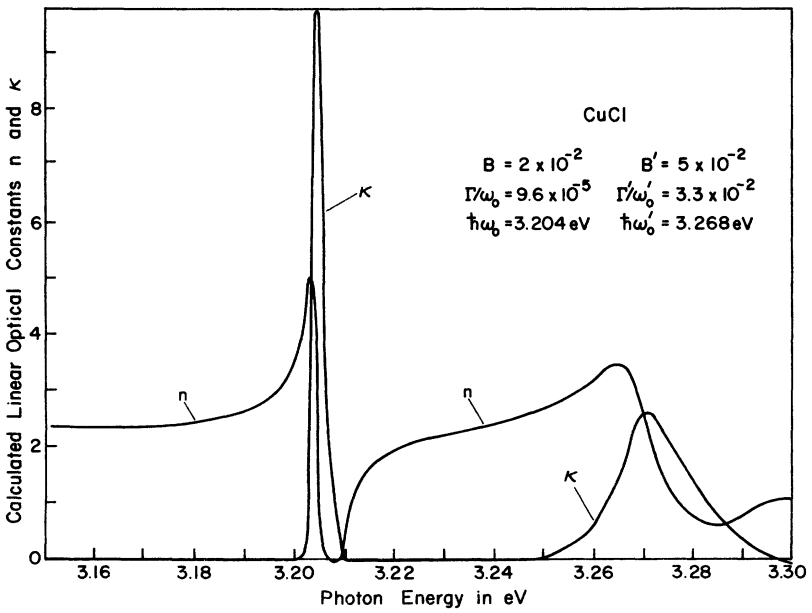

FIG. 11. Linear optical constants of CuCl calculated from the parameters used to make a best fit to SHG data and the linear optical constants calculated from a Kramers-Krönig analysis.

ably be measured well into the excitonic strongly absorbing region of solids.

(b) From second-harmonic generation data in the excitonic region of CuCl and ZnO the resonance behavior of the (lowest-order) nonlinear optical susceptibility d can be deduced. To do this one needs reliable linear optical data in the same region.

(c) A simple anharmonic-oscillator model with two oscillators is able to describe the linear as well as the nonlinear results consistently.

(d) There are two remarks one should add: (i) Small discrepancies between the simple oscillator model and the experimental data, particularly in the vicinity of the first $1s$ exciton in CuCl, are suggestive of possible improvements of the model. (ii) An obvious extension of the model explored here is to include coupling between the oscillators, i.e., spatial dispersion. Such an extension is desirable in principle since it is known that excitons are better described by coupled rather than independent oscillators. This extension of the model will be presented in a separate paper.

ACKNOWLEDGMENTS

Discussions with Professor Hopfield and Professor Tang very much helped to clarify conceptual difficulties. The help of M. Mandell with the computer calculations is acknowledged.

---

†Work supported by the U.S. Office of Naval Research under Contract No. N00014-67-A-0019, Technical Report No. 15, and by the National Science Foundation Grant No. GH-33637 through the Materials Science Center at Cornell University, MSC Report No. 1925.

*Present address: Department of Physics, University of Dallas, Irving, Tex. 75060.

[1]R. K. Chang, J. Ducuing, and N. Bloembergen, Phys. Rev. Lett. **15**, 415 (1965).

[2]W. L. Faust and C. H. Henry, Phys. Rev. Lett. **17**, 1265 (1966).

[3]W. L. Faust, C. H. Henry, and R. H. Eick, Phys. Rev. **173**, 781 (1968).

[4]E. Yablonovitch, N. Bloembergen, and J. J. Wynne, Phys. Rev. B **3**, 2060 (1971).

[5]J. J. Wynne, Phys. Rev. Lett. **27**, 7 (1971).

[6]D. C. Haueisen and H. Mahr, Phys. Rev. Lett. **26**, 838 (1971).

[7]F. G. Parson, E. Y. Chen, and R. K. Chang, Phys. Rev. Lett. **27**, 1436 (1971).

[8]M. D. Levenson, C. Flytzanis, and N. Bloembergen, in Seventh International Quantum Electronic Conference, 1972 (unpublished).

[9]J. A. Armstrong, N. Bloembergen, J. Ducuing, and P. S. Pershan, Phys. Rev. **127**, 1918 (1962).

[10]L. N. Ovander, Usp. Fiz. Nauk **86**, 3 (1965) [Sov. Phys.-Usp. **8**, 337 (1965)].

[11]M. Lang, Phys. Rev. B **2**, 4022 (1970).

[12]N. Bloembergen, *Nonlinear Optics* (Benjamin, New York, 1965), Chap. 1.

[13]S. Nikitine and R. Reiss, J. Phys. Chem. Solids **16**, 237 (1960).

[14]S. Nikitine, *Progress in Semiconductors* (Wiley, New York, 1962), Vol. 6.

[15]M. Cardona, Phys. Rev. **129**, 69 (1963).

[16]F. Raga, R. Kleim, A. Mysyrowicz, J. B. Grun, and S. Nikitine, J. Phys. (Paris) **28**, 3 (1967).

[17]C. Jung, J. Ringeissen, and S. Nikitine, Opt. Commun. **1**, 25 (1969).

[18]A. Feldman and D. Horowitz, J. Opt. Soc. Am. **59**, 1406 (1969).

[19]D. Fröhlich, B. Staginnus, and E. Schönherr, Phys. Rev. Lett. **19**, 1032 (1967).

[20]D. Chemla, P. Kupecek, C. Schwartz, C. Schwab, and A. Goltzene, IEEE J. Quantum Electron. **7**, 126 (1971).

[21]D. G. Thomas, J. Phys. Chem. Solids **15**, 86 (1960).

[22]R. E. Dietz, J. J. Hopfield, and D. G. Thomas, J. Appl. Phys. **32**, 2282 (1961).

[23]J. J. Hopfield and D. G. Thomas, Phys. Rev. Lett. **15**, 22 (1965).

[24]Y. S. Park, C. W. Litton, T. C. Collins, and D. C. Reynolds, Phys. Rev. **143**, 512 (1966).

[25]W. Y. Liang and A. D. Yoffe, Phys. Rev. Lett. **20**, 59 (1968).

[26]Y. S. Park and J. R. Schneider, J. Appl. Phys. **39**, 3049 (1968).

[27]R. Dinges, D. Fröhlich, B. Staginnus, and W. Staude, Phys. Rev. Lett. **25**, 922 (1970); W. Kaule, Solid State Commun. **9**, 17 (1971).

[28]χ and d are macroscopic quantities; for a discussion of local field corrections and the relation of microscopic values of χ and d to the macroscopic ones consult, for example, J. Ducuing and C. Flytzanis, in *Optical Properties of Solids*, edited by F. Abeles (North-Holland, Amsterdam, 1972), Chap. 11, p. 877.

[29]A. Yariv, *Quantum Electronics* (Wiley, New York, 1967), Chap. 21.

[30]N. Bloembergen and P. S. Pershan, Phys. Rev. **128**, 606 (1962).

[31]D. A. Kleinman, Phys. Rev. **128**, 1761 (1962).

[32]R. C. Miller, Appl. Phys. Lett. **5**, 17 (1964).

[33]P. P. Sorokin and J. R. Lankard, IBM J. Res. Dev. **10**, 162 (1966).

[34]Y. Miyazoe and M. Maeda, Appl. Phys. Lett. **12**, 206 (1968).

[35]B. H. Soffer and B. B. McFarland, Appl. Phys. Lett. **10**, 226 (1967).

[36]P. D. Maker, R. W. Terhune, N. Nisenoff, and C. M. Savage, Phys. Rev. Lett. **8**, 21 (1962).

[37]F. C. Jahoda, Phys. Rev. **107**, 1261 (1957).

[38]W. Staude, Phys. Lett. A **29**, 228 (1969). Data plotted are from the computer output of the Kramers-Krönig calculation done by Staude for zero magnetic field in his magnetoreflection study.

[39]D. C. Haueisen and H. Mahr, Phys. Lett. A **36**, 433 (1971).

[40]See Ref. 24. Data plotted are from the computer output of the Kramers-Krönig calculation, provided to the author by Park.

[41]W. L. Bond, J. Appl. Phys. **36**, 1674 (1965).

[42]C. G. B. Garrett, IEEE J. Quantum Electron. **4**, 70 (1968); C. G. B. Garrett and F. N. H. Robinson, IEEE J. Quantum Electron. **2**, 328 (1966).